Anal Bioanal Chem (2011) 399:1151–1162
DOI 10.1007/s00216-010-4369-1

ORIGINAL PAPER

Acridine orange-induced signal enhancement effect of tyrosinase-immobilized carbon-felt-based flow biosensor for highly sensitive detection of monophenolic compounds

Yue Wang · Yasushi Hasebe

Received: 11 September 2010 / Revised: 16 October 2010 / Accepted: 19 October 2010 / Published online: 3 November 2010

Abstract Tyrosinase (TYR: EC 1.14.18.1) was covalently modified onto the surface of a cyanuric chloride-activated carbon felt (CF) from the mixed buffer solution of TYR and acridine orange (AO). The resulting TYR-immobilized CF (TYR/AO-CF) was used as a working electrode unit of an electrochemical flow-through detector for mono- and di-phenolic compounds (i.e., *p*-chlorophenol (*p*-CP), *p*-cresol, phenol, and catechol), which detects the reduction current of enzymatically produced *o*-quinones at −0.05 V (vs. Ag/AgCl). The presence of AO (0.2 mM) in TYR solution during the enzyme immobilization step was significantly effective for the signal enhancements especially for *p*-CP, and the cathodic peak currents of *p*-CP by the TYR/AO-CF-based detector were much larger than those by the TYR-CF-based detector prepared from TYR solution without AO. The oxymetry with Clark-type oxygen electrode revealed that monophenolase activity of free TYR in 1 mM phosphate buffer (pH 7.0) was greatly enhanced in the presence of AO (0.2 mM), whereas diphenolase activity was not so much influenced. Furthermore, the comparison of cyclic voltammograms of TYR/AO-CF and TYR-CF in air-saturated phosphate buffer containing each substrate revealed that the electrochemical reduction rate of *p*-chloro-*o*-benzoquinone at TYR/AO-CF was faster than that at TYR-CF. In addition, the electrochemical impedance spectroscopy revealed that the structural properties of immobilized TYR on the CF would be influenced by AO. Some kinds of interaction of AO with TYR would affect the enzymatic kinetics and the structural properties of the immobilized TYR, leading to the signal enhancement of the TYR-CF-based flow biosensor especially for mono-phenolic compounds.

Keywords Tyrosinase · Acridine orange · Flow biosensor · Carbon felt · Phenolic compounds · Signal enhancement

Y. Wang · Y. Hasebe
Department of Materials Science and Engineering, Graduate School of Engineering, Saitama Institute of Technology,
1690 Fusaiji,
Fukaya, Saitama 369-0293, Japan

Y. Wang
School of Chemical Engineering,
University of Science and Technology Liaoning,
185 Qianshan Road,
Anshan, Liaoning 114044, China

Y. Hasebe (✉)
Department of Life Science and Green Chemistry,
Saitama Institute of Technology,
1690 Fusaiji,
Fukaya, Saitama 369-0293, Japan
e-mail: hasebe@sit.ac.jp

Introduction

Tyrosinase (TYR; polyphenol oxidase, EC 1.14.18.1) is a binuclear copper-containing metalloprotein and possesses two different catalytic activities (i.e., monophenolase activity, ortho-hydroxylation of monophenols, and diphenolase activity, the oxidation of *o*-diphenols to *o*-quinones) [1–5]. On the basis of these activities, a number of TYR-based electrochemical biosensors have been proposed so far for the determination of mono- and di-phenolic compounds [6–21]. In particular, the development of highly sensitive biosensors for mono-phenolic compounds is important research topic because the mono-phenolic compounds are toxic contaminants in ground and surface water.

Most of amperometric TYR-based biosensors detect cathodic current of *o*-quinones produced by the TYR reaction [6–13]. In these sensors, the enzymatically pro-

duced *o*-quinone compounds are electrochemically reduced back to catechol compounds, and the regenerated catechol compounds are re-oxidized by TYR repeatedly. As a result, the enzymatic and the electrochemical recycling of catechol/quinone couple proceeds at the TYR-modified electrode surface, which results in the signal amplification. Thus, the rate-limiting factors of the response of the recycling-based TYR electrodes can be considered as follows: (1) the degree of the catalytic activity of the immobilized TYR, (2) the rate of the electrochemical reduction of *o*-quinone at the electrode surface, and (3) the rate of the mass transfer of oxygen and the diffusion of substrate and product to the electrode surface. Therefore, the performance characteristics of the recycling-based TYR electrodes would be influenced by (1) the TYR immobilization strategy, (2) the microenvironment of the immobilized TYR and the molecular interface between TYR and electrode, and (3) the electrochemical property of the electrode materials.

Carbon felt (CF) is a microelectrode ensemble of microcarbon fiber (ca. 7 μm diameter) and possesses a random three-dimensional structure [22]. The CF has extremely high surface area (estimated to be 0.1 ~ 10 m^2 g^{-1}) and shows high conductivity and high electrolytic efficiency. In addition, high porosity (>90%) and porous structure of the CF causes very low diffusion barrier against solution flow. Therefore, as well as other electroactive porous materials [10, 11, 23–25], the CF is one of the useful candidates of the working electrode unit of the electrochemical flow-through detector and reactor [26, 27]. Therefore, the modification of enzymes on the CF surface would be useful to develop highly functional electrochemical flow biosensors [26, 28–30].

We have recently reported that the OH group on the graphite edge of the CF is useful for the covalent modification of enzyme onto the CF surface [29, 30]. In previous study, the CF surface was first modified with amino-terminated organosilane (i.e., 3-aminopropyltriethoxysilane) via the surface OH group, and then the TYR was covalently modified using various cross-linkers (three step protocol) [29]. More recently, we have proposed more simple TYR modification procedure (two-step protocol) using cyanuric chloride (CC) as a cross-linker between the surface OH group of CF and enzyme [30].

In this study, we found that when the TYR was covalently modified on the CC-activated CF surface from the mixed buffer solution of TYR and acridine orange (AO), the peak current response for monophenolic compound was significantly enhanced as compared with the case without AO in the TYR solution. AO is a polynucleic acid selective fluorescent cationic dye, which interacts with DNA and RNA by intercalation or electrostatic attractions, respectively [31]. However, the interaction of AO with enzyme especially for improving the performance of enzyme-based biosensors has not been reported so far, at least from our best knowledge. The main aim of this study is to find out the role of AO as a signal enhancer of the bioelectrocatalytic activity of the TYR-modified CF and reveal the effectiveness of AO on the peak current responses of the TYR-immobilized CF-based flow biosensor.

Experimental

Reagents and materials

TYR (polyphenol oxidase, EC 1.14.18.1; 5,370 unit/mg from mushroom) was purchased from Sigma Co. (USA) and used as received. AO, phenol, catechol, and cyanuric chloride (CC) were obtained from Wako Pure Chemicals (Osaka, Japan). *p*-Chlorophenol (*p*-CP) and *p*-cresol were obtained from Tokyo Kasei Kogyo Co. (Japan). All of the other chemicals were of the highest grade available and were used without further purifications. Doubly distilled water (Yokozawa Chemical Co., Japan) was used throughout the experiments. Of phosphate buffer solution (pH 7.0), 0.1 M was prepared with K_2HPO_4 and KH_2PO_4. Substrate standard solutions were prepared daily. A CF sheet (GF-20-3F which was prepared by pyrolysis of polyacrylonitrile at 2,000 °C, the density is 1.4 g/cm^3, the porosity is more than 90%) was obtained from Nippon Carbon Ltd. (Japan).

Preparation of the TYR-immobilized CF

The CF sheet was cut into 10×3×3 mm in size (weight, ca. 12 mg), washed with distilled water under ultrasonication for 10 min, and dried in vacuum desiccator for 1 h. The surface activation of the CF by CC and further covalent modification of TYR were carried out according to the method recently reported by us [30]. The CF was immersed into 10 mM CC solution in toluene at room temperature for 1 h. After that, the CF was washed with toluene under ultrasonication for 2 min to remove weakly adsorbed CC, and then dried in vacuum for 1 h. Then, the resulting CC-activated CF was put into 0.1 M phosphate buffer (pH 7.0) solution containing TYR (0.25 mg/ml) and AO (0.2 mM) for 1 h at room temperature. During this procedure, TYR is covalently immobilized on the CF surface via CC [30]. As a control, we prepared the TYR-immobilized CF using TYR-containing 0.1 M phosphate buffer solution without AO. The TYR-immobilized CF prepared from the TYR/AO mixed solution and the TYR solution are denoted here as TYR/AO-CF and TYR-CF, respectively.

Evaluation of the bioelectrocatalytic activity of the TYR/AO-CF and the TYR-CF by cyclic voltammetry (CV)

The cyclic voltammetry (CV) in the presence of each substrate in air-saturated buffer solution was measured to evaluate the bioelectrocatalytic activities (i.e., the activity of immobilized TYR and the electrochemical reduction of *o*-quinones). Air-saturated 0.1 M phosphate buffer (10 ml, pH 7.0) was used as an electrolyte. The TYR/AO-CF and/or the TYR-CF with platinum lead wire were used as working electrode. Auxiliary electrode was platinum wire (1 mm diameter), and reference electrode was Ag/AgCl (BAS, RE-1B). Potential was scanned between +0.5 and −0.3 V at 5 mV/s (starting potential was +0.5 V). Stock solution of substrates (10 mM, 100 μl) was added into the electrolyte (final concentration is ca. 0.1 mM), and then the solution was stirred for 20 s with magnetic stirring bar, and after stop the stirring, the CV was measured at room temperature.

Evaluation of the catalytic activity of free TYR by Clark-type oxygen electrode

To evaluate the effect of AO on the catalytic activities of free TYR in solution, we measured the oxygen consumption rate during the TYR-catalyzed reaction by using Clark-type oxygen electrode (TOA/DKK, Japan) at room temperature. For the assay of the catalytic activity of free TYR, we prepared 30 ml of TYR solution (10 μg/ml) and TYR-AO mixed solution (10 μg/ml TYR and 0.2 mM AO) by dissolving TYR and/or AO in 1 mM phosphate buffer (pH 7.0). The oxygen electrode was immersed in the TYR or TYR/AO solutions placed in 50 ml glass beaker. Throughout the measurement, the potential of −0.7 V (vs. inner reference of the oxygen electrode) was applied to the working electrode under stirring of the solution at constant rate (400 rpm) with magnetic stirring bar. After the background baseline current had reached to the steady-state value (ca. 1.1±0.2 μA), aliquot (180 μL) of the substrate standard solution (0.1 M) was added into the TYR solution (final concentration is ca. 0.6 mM), and the current–time curves were recorded at room temperature.

The electrochemical impedance spectroscopy (EIS) for the evaluation of the interfacial properties of the TYR/AO-CF and the TYR-CF

In order to obtain the interfacial property of TYR/AO-CF and TYR-CF surfaces, the electrochemical impedance spectroscopy (EIS) was carried out with electrochemical analyzer (ALS 6112a) at room temperature. Deoxygenized 0.1 M phosphate buffer solution (15 ml, pH 7.0) containing 1 mM $K_4[Fe(CN)_6]/K_3[Fe(CN)_6]$ as electroactive redox probe was used as an electrolyte. Prior to the measurement, the dissolved oxygen in the buffer was removed by bubbling dry nitrogen gas through the solution at least for 15 min. The EIS measurements were carried out with a conventional one-compartment three-electrode system described above. For the EIS measurement, applied potential was set at formal potential of the redox system (i.e., 0.2 V vs. Ag/AgCl at pH 7.0 in phosphate buffer). The frequency was from 0.01 Hz to 10 kHz.

Amperometric flow injection measurements

Flow injection analysis (FIA) system is composed of a double-plunger pump (DMX 2000T, SNK) with a six-way injection valve (SVM-6M2, SNK, 200 μL injection loop) and the CF-based electrochemical flow-through detector [28–30] connected to the electrochemical analyzer (ALS 611B, USA). All FIA experiments were carried out at room temperature. Air-saturated 0.1 M phosphate buffer (pH 7.0) was used as a carrier solution. Prior to the amperometric measurements, the carrier solution was flowed at constant flow rate of 3.0 ml/min for 1,000 s under the applied potential of −0.05 V vs. Ag/AgCl to remove weakly adsorbed TYR and AO from the CF surface and to reduce the charging background currents. After the background current had reached to steady-state value at −0.05 V vs. Ag/AgCl, 200 μL of substrates standard solution (catechol, *p*-CP, *p*-cresol, and phenol) was injected at regular time intervals, and the cathodic peak currents based on the electrochemical reduction of *o*-quinone species produced by TYR reaction were measured. Although more cathodic potential is effective for the electrochemical reduction of *o*-quinones, it induces the electrochemical reduction of the dissolved oxygen in carrier at the same time. Thus, we selected this potential (−0.05 V vs. Ag/AgCl) to avoid increase in the background current and decrease in the oxygen concentration at the vicinity of the CF surface [6, 7, 29, 30]. To reveal the effect of the presence of AO in sample and carrier solutions, 0.2 mM AO was dissolved in the sample and carrier solutions, and the peak current responses for *p*-CP and catechol were measured in similar way.

Results and discussion

Comparison of the bioelectrocatalytic activities of the TYR/AO-CF and the TYR-CF evaluated by cyclic voltammetry

In order to compare the bioelectrocatalytic behavior of the TYR/AO-CF and the TYR-CF, first we measured cyclic voltammograms (CVs) in air-saturated 0.1 M phosphate buffer (pH 7.0) containing each substrate. Figure 1 compares CVs for 0.1 mM substrates (*p*-CP, *p*-cresol, phenol,

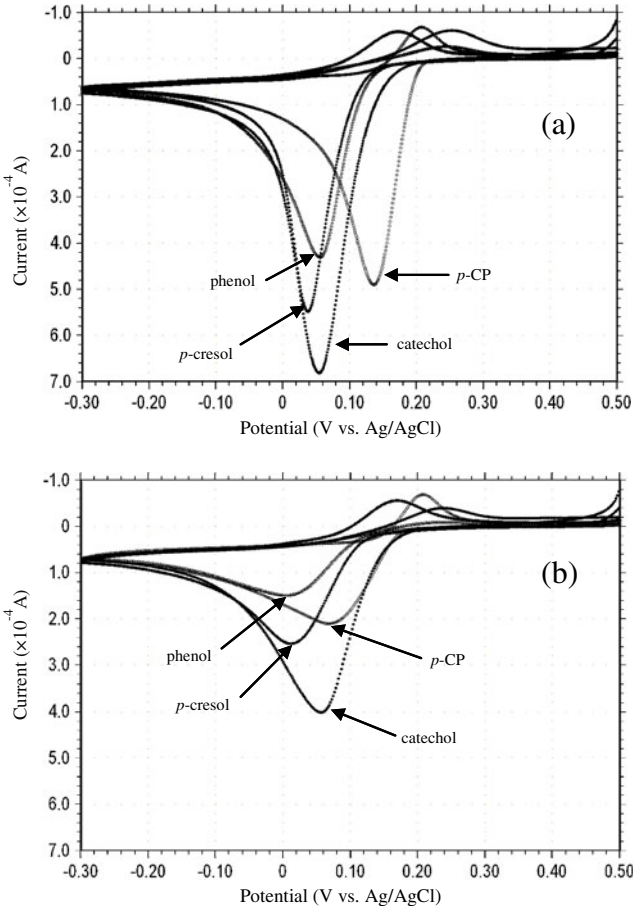

Fig. 1 Cyclic voltammograms (CVs) of the (**a**) TYR/AO-CF and (**b**) TYR-CF in air-saturated 0.1 M phosphate buffer (pH 7.0) containing 0.1 mM TYR substrates (*p*-CP, *p*-cresol, phenol, and catechol). Potential scan rate is 5 mV/s. Starting potential is +0.5 V

and catechol) recorded at 5 mV/s at the TYR/AO-CF (a) and at the TYR-CF (b). Table 1 summarizes the electrochemical parameters of the CVs. For every substrate, both TYR/AO-CF (a) and TYR-CF (b) exhibited larger cathodic currents than anodic currents, which are typical shapes of catalytic wave, due to the repetitive reduction of *o*-quinone species produced by the TYR-catalyzed oxidation. Thus, the magnitude of this cathodic current can be the parameter to evaluate the bioelectrocatalytic activity of TYR-modified CF. The TYR/AO-CF (a) exhibited enhanced reduction currents (catalytic currents) for every substrate in comparison with the TYR-CF (b). These results indicate that the presence of AO in the TYR immobilization step was effective to enhance the bioelectrocatalytic activity of the TYR-modified CF.

Table 1 Electrochemical parameters of CVs with the shape of catalytic wave

CF	Substrate	E_c	E_a	ΔE	I_c	I_a
		mV			μA	
TYR/AO-CF	*p*-chlorophenol	136	208	72	−488	104
	p-cresol	38	173	135	−537	84
	phenol	55	245	190	−421	35
	catechol	55	253	198	−666	66
TYR-CF	*p*-chlorophenol	69	208	139	−208	98
	p-cresol	11	169	158	−236	83
	phenol	5	239	234	−136	34
	catechol	57	239	182	−389	58

E_c cathodic peak potential, E_a anodic peak potential, I_c cathodic peak current, I_a anodic peak current

As described in the "Introduction" section, the bioelectrocatalytic response of the present recycling-based TYR electrode originated from the bioelectrocatalytic cycle driven by the TYR-catalyzed oxidation of phenolic compounds producing *o*-quinones and the electrochemical reduction of *o*-quinones. Therefore, the rate of the electrochemical reduction of *o*-quinone species is also an important parameter influencing the response characteristics of the redox-recycling-based TYR electrodes [20, 21]. Especially, in the case of *p*-CP response, the TYR/AO-CF showed cathodic and anodic peaks at 136 and 208 mV, respectively (5 mV/s vs. Ag/AgCl), while the TYR-CF showed cathodic and anodic peaks at 69 and 208 mV, respectively. As a result, the TYR/AO-CF and the TYR-CF have the peak-to-peak separation (ΔE) of 72 and 139 mV, respectively. These results suggest that electron transfer rate of the electrochemical reduction of *p*-chloro-*o*-benzoquinone at the TYR/AO-CF is faster than that at the TYR-CF.

Since AO does not possess any functional group for the covalent bonding via CC, it can be safe to assume that the interactions of AO with TYR and/or CF surface not only enhance the catalytic activity of the adsorbed TYR but also facilitate the electron transfer of *p*-chloro-*o*-benzoquinone at the TYR/AO-CF surface.

Effect of AO on monophenolase and diphenolase activity of free TYR in solution phase

As described in the "Introduction" section, one of the rate-limiting factors of this sensor is the degree of the catalytic activity of the immobilized TYR. Therefore, it would be reasonable to assume that the interaction of AO with TYR would cause the change of the catalytic activity of TYR itself. Figure 2 shows the proposed catalytic cycle of monophenolase and diphenolase activities of TYR [2]. TYR has three forms (i.e., met, oxy, and deoxy) of the active sites. According to this scheme, in both monophenolase and diphenolase cycles, the molecular oxygen is introduced to the active copper center of TYR when the oxy-form is produced from the deoxy-form. Thus, the assay of the oxygen consumption rate can be used for the study of the TYR reaction kinetics [32]. Therefore, to evaluate the effect of AO on the catalytic activities of TYR, we

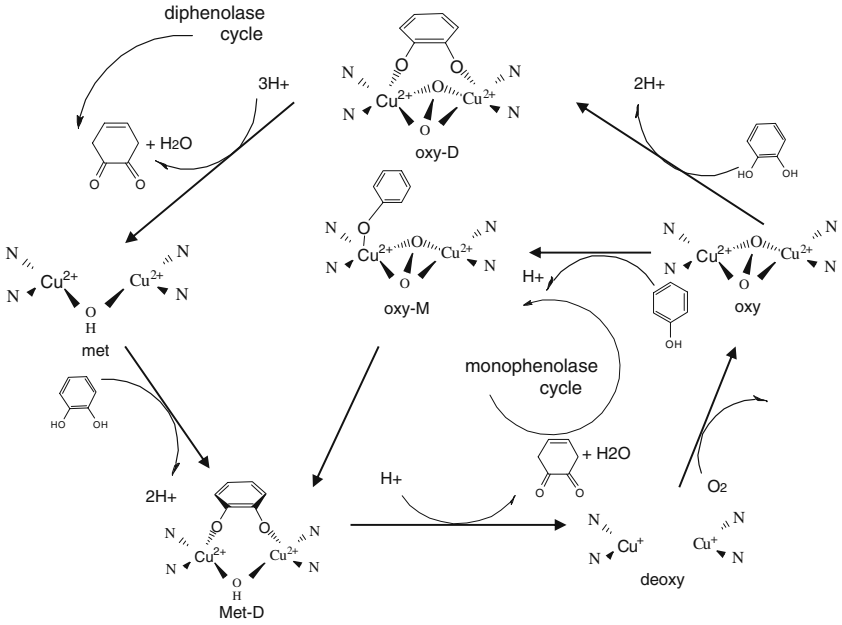

Fig. 2 Catalytic cycle for the mono-oxygenation of monophenols and the oxidation of *o*-diphenols to *o*-quinones by tyrosinase. Axial ligands at Cu not included for clarity. *M* monophenol compounds, *D* diphenol compounds [2]

compared the O_2 consumption rate using Clark-type oxygen electrode in TYR solution with and without 0.2 mM AO.

Figure 3 shows the results of the oxymetry, i.e., the relationship between the residual O_2 (percent) and the reaction time after the addition of the substrates. In general, the oxygenation reaction based on monophenolase activity ($K_{\text{diphenaolase}}=10^3\ s^{-1}$) is much slower than the oxidase reaction based on diphenolase activity ($K_{\text{monophenaolase}}=10^7\ s^{-1}$) [33] because only small portions of the active site of TYR can catalyze the ortho-hydroxylation reaction of

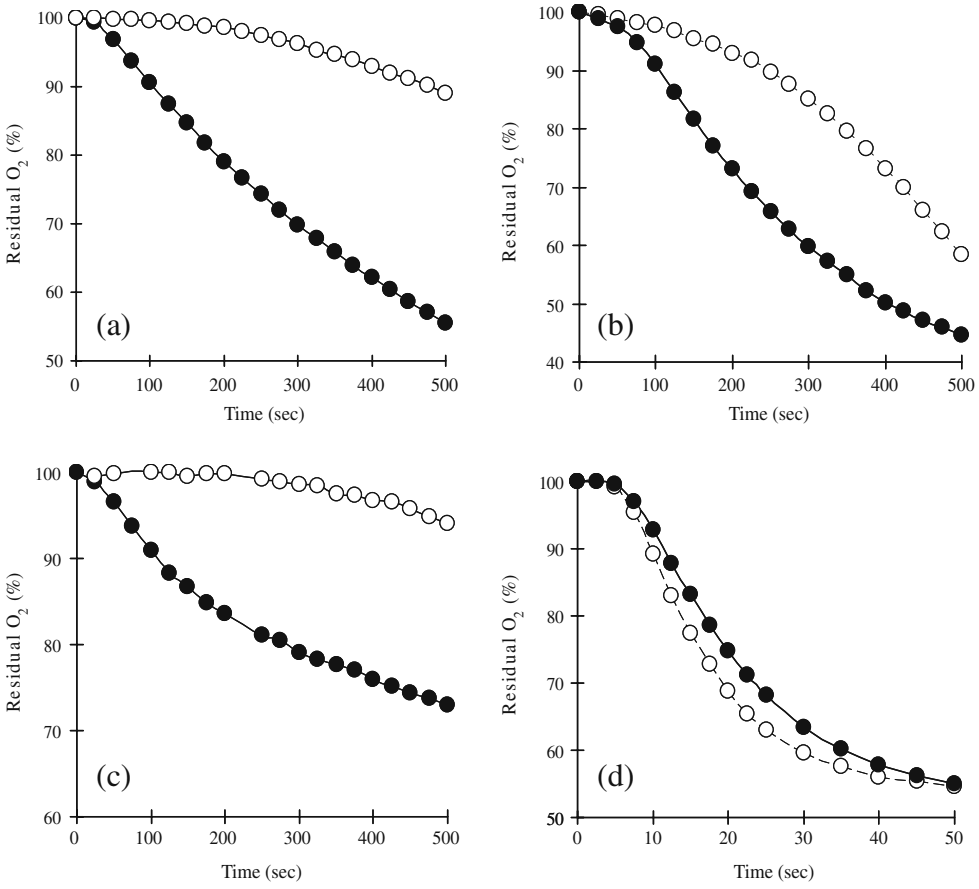

Fig. 3 Time course of O_2 consumption in the oxidation of (**a**) *p*-CP, (**b**) *p*-cresol, (**c**) phenol, and (**d**) catechol in the presence (*closed circles*) and absence (*open circles*) of 0.2 mM AO in 1 mM phosphate buffer (pH 7.0) containing TYR (10 μg/ml). Concentration of each substrate is 0.6 mM. Temperature is room temperature

monophenolic compounds in resting state [34, 35]. In fact, in the absence of AO, the oxygen consumption rates in the oxygenation reaction of monophenolic compounds such as *p*-CP (a), *p*-cresol (b), and phenol (c) were much smaller than that of catechol (d). However, the oxygen consumption rates in the oxidation of monophenolic compounds were significantly increased in the presence of AO. In addition, the lag period of monophenolase activity seemed to be shortened in the presence of AO. In contrast, in the case of catechol (d), the rate of oxygen consumption was not so much influenced by AO. These results clearly indicate that the monophenolase activity of TYR in solution phase was greatly enhanced in the presence of 0.2 mM AO. Therefore, at least from this result, it can be safe to assume that AO can interact with TYR and alter the catalytic activity of TYR.

It has been reported that appropriate reducing reagents such as dithiothreitol (DTT) and ascorbic acid accelerate the transformation of met-form of TYR to deoxy-form of TYR (see Fig. 2), which leads to the enhancement of the monophenolase activity and shortening the lag period [35, 36]. However, in our case, differing from DTT and ascorbic acid, AO is not redox active. Thus, it would be safe to assume that some kinds of interactions between AO and TYR might cause the structural change of TYR, which leads to the enhancement of the monophenolase activity. As shown in Fig. 2, in the monophenolase cycle, the monophenol compounds bind to the axial position of one of the coppers of the oxy-site and undergo a trigonal bipyramidal rearrangement toward the equatorial plane which orients its ortho-position for hydroxylation. This generates a coordinated *o*-diphenolate, which is oxidized to the quinone, resulting in a deoxy site ready for further dioxygen binding [1]. Thus, it would be possible to speculate that AO can accelerate the rearrangement at the copper site for simple electron transfer for phenol compounds. However, the details of the mechanism of this AO-induced activation of monophenolase activity and the interaction between AO and TYR are unfortunately not clear in this stage. Further study from the different points of view would be required to reveal these phenomena, and these studies are now under progress, and the results would be reported in another paper.

Comparison of the interfacial properties of the TYR/AO-CF and the TYR-CF evaluated by electrochemical impedance spectroscopy

In general, the activity of immobilized enzyme is significantly affected by the conformation and the structure of enzyme on the matrix surface. The formation of the chemical bonding or various interactions between the enzyme and matrix surface (e.g., electrostatic, hydrophobic, and van der Waals interactions) sometimes cause the conformational and the structural changes of the enzyme, which may lead to the change of the enzymatic activity [37, 38]. As can be seen in Fig. 3d, AO does not influence so much to the catalytic activity of free TYR for catechol oxidation (diphenolase activity) in solution phase. However, as can be seen in Fig. 1a, b, the bioelectrocatalytic activity of the TYR/AO-CF for catechol oxidation was enhanced clearly in comparison with the TYR-CF. In addition, the oxygen consumption rate due to the catechol oxidation by the TYR/AO-CF (which is measured with oxygen electrode equipped with TYR/AO-CF) was about twice by the TYR-CF (data not shown), indicating that the diphenolase activity of the TYR/AO-CF was larger than that of the TYR-CF. These facts suggest the possibility that the interaction of AO with TYR affects the structural properties of the immobilized TYR layer, such as density, defects, conformation, and orientation, which would result in the difference in the activity of immobilized TYR.

EIS using small redox couples (e.g., $Fe(CN)_6^{4-/3-}$) is a powerful tool for studying the interfacial properties of the surface-modified electrodes [39, 40]. Figure 4 shows the Nyquist plots of EIS for TYR/AO-CF (curve a) and TYR-CF (curve b). The electron transfer resistance (R_{CT}) at the electrode surface, which can be estimated by the Nyquist diameter, is an important parameter. The estimated R_{CT} of the TYR/AO-CF (curve a≈35 Ω) was smaller than that of the TYR-CF (curve b≈60 Ω). Based on the assumption that (1) the electro-active species (in this case, $Fe(CN)_6^{4-/3-}$)

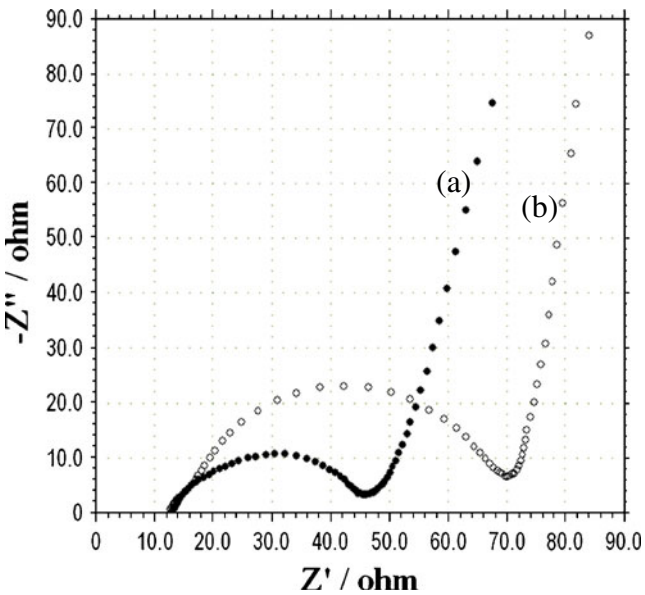

Fig. 4 Nyquist plots of electrochemical impedance spectroscopy (EIS) for (*a*) TYR/AO-CF and (*b*) TYR-CF. Electrolyte is deoxygenized 0.1 M phosphate buffer containing 1 mM $Fe(CN)_6^{4-/3-}$ (pH 7.0). Applied potential was set at formal potential of the redox system (i.e., 0.2 V vs. Ag/AgCl). The frequency is from 0.01 Hz to 10 kHz

could directly diffuse to the bare spots on the CF through pores and defects of the immobilized TYR layer and (2) the electro-active species could permeate through the immobilized TYR layer and react at the CF surface, the difference in the R_{CT} between the TYR/AO-CF and the TYR-CF would be attributed to the difference in the covered area of the TYR layer and/or the structural properties of the TYR layer on the CF surface.

It has been reported that 1-anilino-8-naphthalene sulfonate (ANS) binds to some proteins through the electrostatic interaction between the negatively charged sulfonate group of ANS and the cationic groups of the proteins, and that the ANS acts as a conformational tightening agent of protein [41]. In addition, it is generally known that the structure and the conformational flexibility of proteins are changed by ligand interactions [42, 43]. In the case of glucose oxidase, monovalent cations (such as K^+, Na^+, and Cs^+) bind to negatively charged group of GOx and stabilize the enzyme against urea-induced and thermal denaturations [44]. Furthermore, this cation-stabilized GOx has more compact structure based on the change of tertiary structure [44]. The isoelectric point (I_p) of TYR is 4.7 [45], and AO has a positive charge at neutral pH condition. Considering the above phenomena and our results, it would be reasonable to speculate that the electrostatic interaction between AO and the anionic groups of TYR may contribute to the difference of the structural properties of the immobilized TYR. Based on the assumption that the partial denaturation could be induced by the chemical modification of TYR onto the CC-activated CF surface, the AO-bound TYR shows the resistance to partial denaturation, resulting in the enhanced diphenolase activity as well as the monophenolase activity. Namely, the difference in the structural properties of the immobilized TYR on the CF surface between the TYR/AO-CF and the TYR-CF may also likely reflect the difference in the catalytic activity of the immobilized TYR.

From these results, it can be considered that the following three kinds of functions of AO would influence the bioelectrocatalytic activity of the TYR-modified CF: (1) the activation of monophenolase activity, (2) the facilitation of the electrochemical reduction of *o*-quinone, and (3) the stabilizing effect against the surface- or chemical modification-induced partial denaturation. However, among them, the activation of the enzymatic activity (phenolase activity) seems to be a primary factor for the signal enhancement of monophenolic compounds by this system.

Comparison of the peak current responses of the TYR/AO-CF- and the TYR-CF-based flow biosensors

Next, we studied the peak current response characteristic of the TYR-immobilized CF-based flow biosensor. We measured the cathodic peak current responses of three monophenolic compounds (i.e., *p*-chlorophenol, *p*-cresol, and phenol) and catechol, and compared the responses of the TYR/AO-CF- and the TYR-CF-based flow biosensors.

In order to obtain highly sensitive peak current responses, first we optimized the AO concentration and applied potential using *p*-CP as a model substrate. Figure 5a shows the effect of AO concentration in TYR solution during the enzyme immobilization step upon the cathodic peak current response of *p*-CP (10 μM). Peak current responses were increased with increasing of AO concentration and seemed to reach plateau at around 0.2 mM. This result clearly indicates that AO is essential to enhance the bioelectrocatalytic activity of TYR-modified CF. Based on

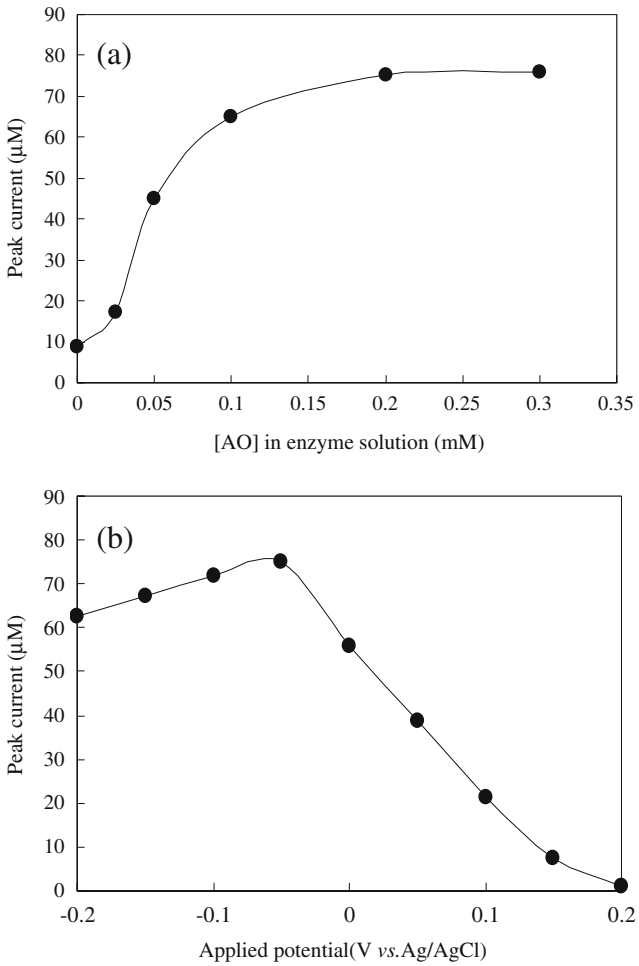

Fig. 5 (**a**) Effect of AO concentration in TYR solutions during the enzyme immobilization step upon the peak current responses to 10 μM *p*-CP. Applied potential is −0.05 V vs. Ag/AgCl. Carrier solution is air-saturated 0.1 M phosphate buffer (pH 7.0). Carrier flow rate is 3.0 ml/min. Measurements were performed at room temperature. (**b**) Effect of applied potential on the peak current responses to 10 μM *p*-CP. The measurement conditions (except for the applied potential) are same in (**a**)

this result, 0.2 mM was selected as an optimum AO concentration for most of the experiments.

Figure 5b shows the effect of applied potential upon the peak current of 10 μM *p*-CP. Cathodic peak current appeared at +0.15 V and increased with changing the potential from +0.15 to −0.05 V, and the maximum value was observed at −0.05 vs. Ag/AgCl. Gradual decrease in peak current in more negative potential region (from −0.1 to −0.2 V) would be attributed to the increased background current, which is probably due to the reduction of dissolved oxygen in carrier. Thus, we selected −0.05 V vs. Ag/AgCl as an optimum applied potential of the TYR-CF-based flow biosensor.

Figure 6 shows typical peak current responses of *p*-CP obtained by (a) the TYR/AO-CF- and (b) the TYR-CF-based flow biosensors. It is clear that the TYR/AO-CF-based flow biosensor exhibited larger responses than the TYR-CF-based biosensor. In addition, the TYR/AO-CF-based biosensor showed apparent responses toward 10 nM *p*-CP (inset graph of panel a), while the TYR-CF-based biosensor did not show clear response toward same concentration of *p*-CP (data not shown). However, there was no significant difference in the background current (baseline) and the signal noise level between the TYR/AO-CF- and the TYR-CF-based biosensors. In both biosensors, RSD (n=3) for the measurements of same concentration of standard samples was relatively good, and the RSD values were in the range from 0.33 to 3.7.

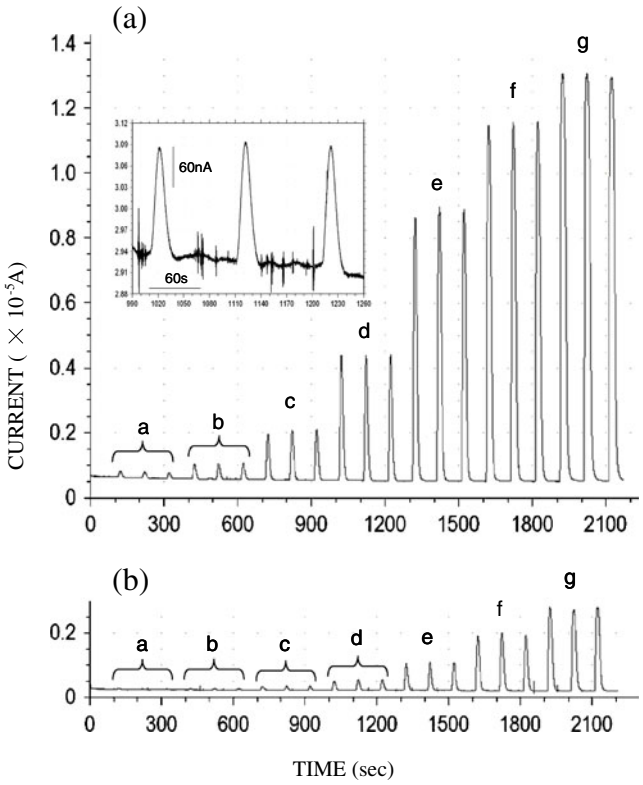

Fig. 6 Typical peak current responses for *p*-CP obtained by the (**a**) TYR/AO-CF and (**b**) TYR-CF-based flow biosensors. Concentration of *p*-CP: *a* 0.1, *b* 0.3, *c* 1, *d* 3, *e* 10, *f* 30, *g* 100 μM. Applied potential is −0.05 V vs. Ag/AgCl. Carrier solution is air-saturated 0.1 M phosphate buffer (pH 7.0). Carrier flow rate is 3.0 ml/min. Measurements were performed at room temperature. *Inset graph* of panel **a**: peak current response for 10 nM *p*-CP obtained by the TYR/AO-CF-based flow biosensor

Next, we studied the effect of AO in sample and carrier solutions on the cathodic peak current response of *p*-CP. Figure 7 shows relative peak responses obtained by the TYR-CF and the TYR/AO-CF with and without 0.2 mM AO in sample and carrier solutions. In the case of the TYR-CF-based biosensor (bar a and b), the peak current response of *p*-CP (30 μM) obtained by using AO-containing sample and carrier (bar b) was about two times as large as that obtained without AO (bar a). On the other hand, in the case of the TYR/AO-CF (bar c and d), the response with AO-containing sample and carrier was about 1.3 times as large (bar d) as that without AO (bar c). These results suggest that AO in sample and carrier was also effective for the signal enhancement of *p*-CP. In other words, AO is still effective to already immobilized TYR. However, by the comparison of the responses of the TYR/AO-CF (bar c and d) and the TYR-CF (bar a and b), it is clear that the presence of AO in TYR solution during the enzyme immobilization step is much effective as compared with the presence of AO in sample and carrier solutions during the measurements.

Figure 8 shows the calibration curves for (a) *p*-CP, (b) *p*-cresol, (c) phenol, and (d) catechol obtained by (closed squares) TYR/AO-CF- and (open squares) TYR-CF-based flow biosensors. Tables 2 and 3 summarize the performance

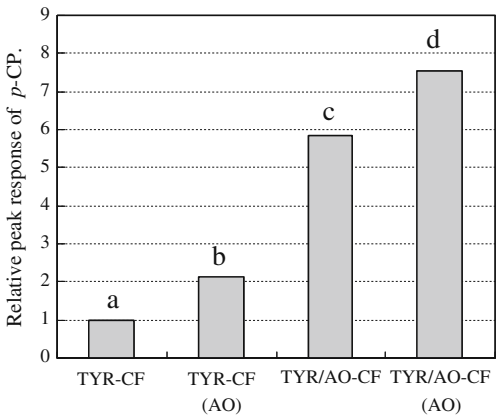

Fig. 7 Comparison of peak current responses of 30 μM *p*-CP (relative value), obtained by the TYR-CF (bar *a*, *b*) and the TYR/AO-CF (bar *c*, *d*) in the absence (bar *a*, *c*) and the presence (bar *b*, *d*) of 0.2 mM AO in sample and carrier solutions. Other experimental conditions are same in Fig. 6

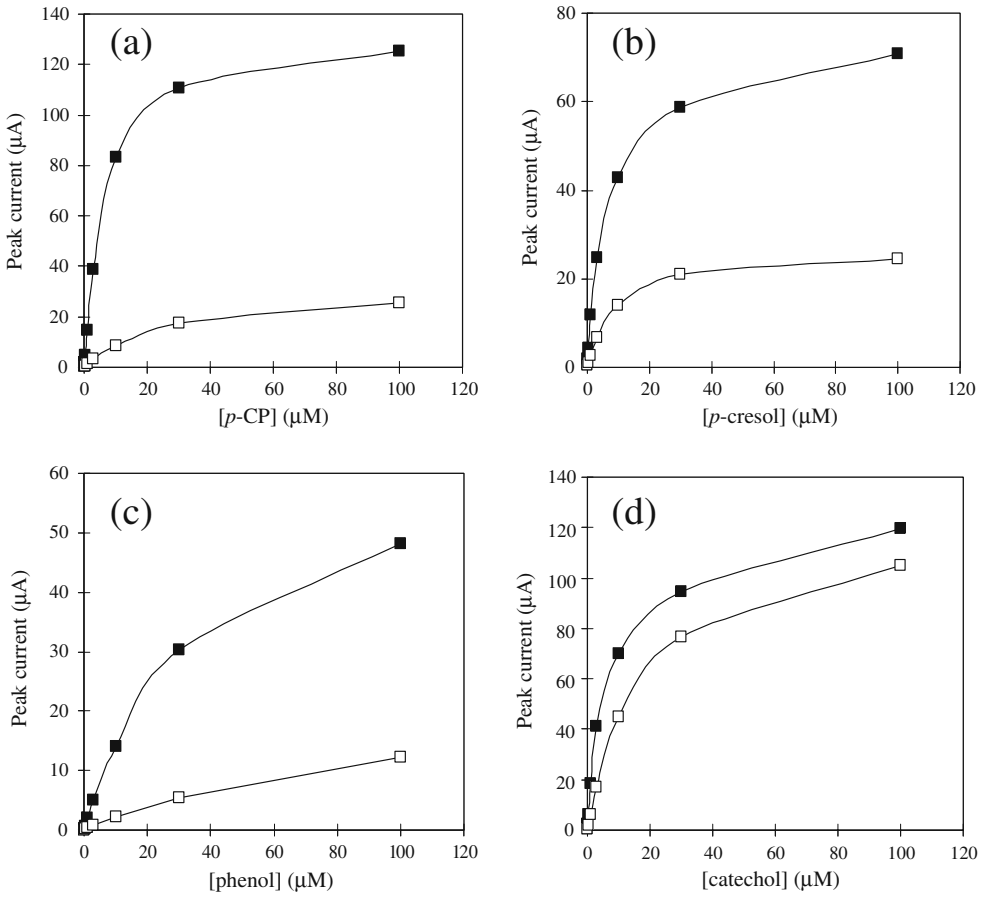

Fig. 8 Calibration curves of (**a**) *p*-CP, (**b**) *p*-cresol, (**c**) phenol, and (**d**) catechol obtained by the (*closed squares*) TYR/AO-CF- and (*open squares*) TYR-CF-based flow biosensors. Experimental conditions are same in Fig. 6

characteristics (i.e., the sensitivity, the lower detection limit, apparent K_m, I_{max}, and the linear range of the calibration curve) of the TYR/AO-CF- and the TYR-CF-based biosensors, respectively. Judging from the shape of the calibration curves, the signal enhancement effect by AO seems to be more remarkable for monophenolic compounds as compared with catechol. For example, the sensitivities (i.e., the slope of the linear portion of the calibration curve) of *p*-CP, *p*-cresol, and phenol by the TYR/AO-CF-based biosensor were about 12, 5, and 8 times as high as those by the TYR-CF-based biosensor, respectively, while the sensitivity of catechol by the TYR/AO-CF-based biosensor was only 2.3 times as high as that by the TYR-CF-based biosensor. As a result, the lower detection limits of *p*-CP, *p*-cresol, and phenol by the TYR/AO-CF-based biosensor decreased about one order of magnitude as compared with the TYR-CF-based biosensor, and the lower detection limit of *p*-CP and *p*-cresol decreased to nanomolar level. In addition, the I_{max} values of monophenolic compounds by the TYR/AO-CF-based biosensor were about three to four times as large as those by the TYR-CF-based biosensor, while the I_{max} value of catechol by the TYR/AO-CF-based biosensor was almost the same as that by

Table 2 Performance characteristics of the TYR/AO-CF-based flow biosensors

Analytes	TYR/AO-CF					
	Sensitivity[a] μA/μM	Detection limit[b] nM	K_m μM	I_{max} μA	Linear range M	Linearity R^2
p-chlorophenol	11.8	2.6	5.9	149	2.6×10^{-9}–3×10^{-6}	0.9996
p-cresol	11.2	2.7	7.5	75	2.7×10^{-9}–1×10^{-6}	0.9993
Phenol	1.6	18.7	37.9	68	1.9×10^{-8}–1×10^{-5}	0.9976
Catechol	13.2	2.3	8.0	125	2.3×10^{-9}–3×10^{-6}	0.9893

[a] Slope of the linear portion of calibration curve

[b] Noise level, 10 nA (S/N=3)

Table 3 Performance characteristics of the TYR-CF-based flow biosensors

Analytes	TYR-CF					
	Sensitivity[a] μA/μM	Detection limit[b] nM	K_m μM	I_{max} μA	Linear range M	Linearity R^2
p-chlorophenol	0.99	30	31.3	34	3.0×10^{-8}–1×10^{-5}	0.9722
p-cresol	2.1	14	8.9	27	1.4×10^{-8}–3×10^{-6}	0.9955
Phenol	0.2	143	93.3	23	1.4×10^{-7}–3×10^{-5}	0.9951
Catechol	5.7	5.3	17.1	122	5.3×10^{-9}–1×10^{-5}	0.9994

[a] Slope of the linear portion of calibration curve

[b] Noise level, 10 nA (S/N=3)

the TYR-CF-based sensor. Furthermore, the K_m values of all substrates obtained by the TYR/AO-CF-based biosensor were smaller than those by the TYR-CF-based biosensor. These results indicate that the presence of AO in TYR solution during the enzyme immobilization step is considerably useful to enhance the cathodic peak current response of monophenolic compounds, especially *p*-CP.

TYR has broad specificity toward various mono- and diphenolic compounds, and substrate selectivity of TYR is usually the following trends: catechol≫*p*-cresol>*p*-CP> phenol [6, 11, 18]. In this study, we used the sensitivity as an indication of the selectivity toward various phenolic compounds because the sensitivity reflects the bioelectrocatalytic activity of the present TYR-modified CF-based flow detector. In fact, the trend in the sensitivity by the TYR-CF-based biosensor was catechol≫*p*-cresol≫*p*-CP> phenol. However, in the case of the TYR/AO-CF-based biosensor, the sensitivities of *p*-CP and *p*-cresol were greatly enhanced, while the sensitivity of catechol was not so much changed. As a result, the TYR/AO-CF-based biosensor showed almost the same sensitivities toward *p*-CP, *p*-cresol, and catechol. This means that AO is useful to not only enhance the sensitivity but also alter the selectivity of the TYR-immobilized CF-based biosensor. The change in the selectivity pattern (*p*-cresol>catechol) was observed when TYR was incorporated into hydrophobic graphite-epoxy resin matrix [7]. The sensitivity of *p*-CP by our system seemed to be superior to other TYR-based biosensors using graphite-epoxy resin matrix [7], TYR-modified reticulated vitreous carbon [10], poly-L-lysine-coated porous stainless steel [11], cation-exchanger film-coated graphite electrode [19], and covalently modified TYR on amino-functionalized CF [29].

The operational stability of the TYR/AO-CF-based biosensor was checked by consecutive ten injections of 1 μM *p*-CP. Relative standard deviation (RSD) was 1.74 (n=10). In some cases, the oxidation products and the polymerized products from *o*-quinones cause the inactivation of TYR and/or an electrode fouling, resulting in less operational stability [6, 7, 12, 19, 29]. However, the resulting TYR/AO-CF-based flow biosensor exhibited excellent operational stability at least for the measurements of 1 μM concentration level of *p*-CP.

The reproducibility of the peak current responses obtained from different TYR/AO-CF constructed in the same manner is an essential aspect to be evaluated in order to assess the practical usefulness of the developed amperometric biosensor. Three electrodes were fabricated in the same manner, and amperometric measurements for calibration curves of *p*-CP were carried out with each electrode. The RSD value for the sensitivity (the slope of the linear part of the calibration curve) of the three TYR/AO-CF electrodes for *p*-CP measurement was 3.1%, indicating that the fabrication procedure of the TYR/AO-CF electrodes was reliable, and that reproducible electrochemical peak responses can be achieved with different TYR/AO-CF electrodes constructed in the same manner.

Conclusions

In this study, we found that the presence of AO in TYR solution during the enzyme immobilization step is significantly effective to enhance the peak current response of the TYR-immobilized CF-based flow biosensor especially for monophenolic compounds, which detect cathodic current of electrochemical reduction of *o*-quinone species produced by the TYR-catalyzed reaction. For the responses of monophenolic compounds (especially *p*-CP), the following three kinds of functions of AO would synergistically lead to the signal enhancements: (1) the activation of monophenolase activity, (2) the facilitation of the electrochemical reduction of *o*-quinone, and (3) the stabilizing effect against the surface- or chemical modification-induced partial denaturation. Among them, the activation of the enzymatic activity (phenolase activity) seems to be a primary factor for the signal enhancement of monophenolic compounds by this system. On the other hand, for catechol response, the stabilizing effect against the partial denaturation would be the primary reason of the signal enhancement. Because of the broad selectivity toward various mono- and di-phenolic compounds, the TYR-modified CF-based flow biosensors must be useful for continuous monitoring of highly toxic phenol compounds and clinically important catecholamines. Further studies on the interaction between AO and TYR are now in progress.

Acknowledgements This research was financially supported in part by the Open Research Center Project of the Ministry of Education, Science, and Culture of Japan.

References

1. Wilcox DE, Porras AG, Hwang YT, Lerch K, Winkler ME, Solomon EI (1985) Substrate analog binding to the coupled binuclear copper active site in tyrosinase. J Am Chem Soc 107:4015–4027
2. Solomon EI, Sundaram UM, Machonkin TE (1996) Multicopper oxidases and oxygenases. Chem Rev 96:2563–2606
3. García-Molina F, Muñoz JL, Varón R, Rodríguez-López JN, García-Cánovas F, Tudela J (2007) A review on spectrophotometric methods for measuring the monophenolase and diphenolase activities of tyrosinase. J Agric Food Chem 55:9739–9749
4. Vanneste WH, Zuberbuhler A (1974) Copper containing oxygenases. In: Nayaishi O (ed) Molecular mechanism of oxygen activation. Academic, New York
5. Lerch K (1981) Copper monooxygenases: tyrosinase and dopamine β-monooxygenase. In: Sigel H (ed) Metal ions in biological systems. Dekker, New York
6. Ortega F, Dominguez E, Jönsson-Petterson G, Gorton L (1993) Amperometric biosensor for the determination of phenolic compounds using a tyrosinase graphite electrode in a flow injection system. J Biotechnol 31:289–300
7. Wang J, Fang L, Lopez D (1994) Amperometric biosensor for phenols based on a tyrosinase-graphite-epoxy biocomposite. Analyst 119:455–458
8. Onnerfjord P, Emnesu J, Marko-Varga G, Gorton L, Ortega F, Dominguez E (1995) Tyrsosinase graphite-epoxy based composite electrodes for detection of phenols. Biosens Bioelectron 10:607–619
9. Wang B, Dong S (2000) Organic-phase enzyme electrode for phenolic determination based on a functionalized sol-gel composite. J Electroanal Chem 487:45–50
10. Peña N, Reiviejo AJ, Pingarron JM (2001) Detection of phenolic compounds in flow systems based on tyrosinase-modified reticulated vitreous carbon electrodes. Talanta 55:179–187
11. Ducey MW Jr, Meyerhoff ME (1998) Microporous gold electrodes as combined biosensor/electrochemical detectors in flowing streams. Electroanalysis 10:157–162
12. Ortega F, Domínguez E, Burestedt E, Emnéus J, Gorton L, Marko-Varga G (1994) Phenol oxidase-based biosensors as selective detection units in column liquid chromatography for the determination of phenolic compounds. J Chromatogr A 675:65–78
13. Liu Z, Liu Y, Yang H, Yang Y, Shen G, Yu R (2005) A phenol biosensor based on immobilizing tyrosinase to modified core-shell magnetic nanoparticles supported at carbon paste electrode. Anal Chim Acta 533:3–9
14. Lutz M, Burestedt E, Emnéus J, Lindén H, Gobhadi S, Gorton L, Marko-Varga G (1995) Effect of different additives on a tyrosinase based carbon paste electrode. Anal Chim Acta 305:8–17
15. Liu A, Hnma I, Zhou H (2005) Amperometric biosensor based on tyrsinase-conjugated polysaccharide hybrid film: selective determination of nanomolar neourotransmitters metabolite of 3,4-dihydroxyphenylacetic acid (DOPAC) in biological fluid. Biosens Bioelectron 21:809–816
16. Liu S, Yu J, Ju H (2003) Renewable phenol biosensor based on a tyrosinase-collodal gold modified carbon paste electrode. J Electroanal Chem 540:61–67
17. Wang J, Lu F, Kane SA, Choi YK, Smyth MR, Rogers K (1997) Hydrocarbon pasting liquids for improved tyrosinase-based carbon paste phenol biosensors. Electroanalysis 9:1102–1106
18. Marko-Varga G, Burestedt E, Svensson CJ, Emneus J, Ruzgas T, Lutz M, Unger KK (1996) Effect of HY-Zeolites on the performance of tyrosinase-modified carbon paste electrodes. Electroanalysis 8:1121–1126
19. Nistor C, Emnéus J, Gorton L, Ciucu A (1999) Improved stability and altered selectivity of tyrosinase based graphite electrodes for detection of phenolic compounds. Anal Chim Acta 387:309–326
20. Burestedt E, Narvaesz A, Ruzgas T, Gorton L, Emnéus J, Domínguez E, Marko-Valma G (1996) Rate-limiting steps of tyrosinase-modified electrodes for the detection of catechol. Anal Chem 68:1605–1611
21. Hedenmo M, Narváez A, Domínguez E, Katakis I (1997) Improved mediated tyrosinase amperometric enzyme electrodes. J Electroanal Chem 425:1–11
22. Kato K, Kano K, Ikeda T (2000) Electrochemical characterization of carbon felt electrodes for bulk electrolysis and for biocatalyst-assisted electrolysis. J Electrochem Soc 147:1449–1453
23. Blaedel WJ, Wang J (1979) Flow analysis on reticulated vitreous carbon electrode. Anal Chem 51:799–802
24. Strohl AN, Curran DJ (1979) Flow injection analysis with reticulated vitreous carbon flow-through electrodes. Anal Chem 51:1045–1049
25. Khayyami M, Johansson G, Kriz D, Xie B, Larsson PO, Danielsson B (1996) Flow-injection determination of race hydrogen peroxide or glucose utilizing an amperometric biosensor based on glucose oxidase bound to a reticulated vitreous carbon electrode. Talanta 43:957–962
26. Rödel U, Geschke O, Cammann K (1996) Entrapment of enzyme in electropolymers for biosensors and graphite felt based flow-through enzyme reactors. Electroanalysis 8:1135–1139
27. González-García J, Montiel V, Aldaz A, Conesa JA, Pérez JR, Codina G (1998) Hydrodynamic behavior of a filter-press electrochemical reactor with carbon felt as a three dimensional electrode. Ind Eng Chem Res 37:4501–4511
28. Hasebe Y, Imai R, Hirono M, Uchiyama S (2007) Carbon felt-based bioelectrocatalytic flow detectors: highly sensitive amperometric determination of hydrogen peroxide using adsorbed peroxidase and thionine. Anal Sci 23:71–74
29. Wang Y, Hasebe Y (2009) Carbon felt-based biocatalytic enzymatic flow-through detectors: chemical modification of tyrosinase onto amino-functionalized carbon felt using various coupling reagents. Talanta 79:1135–1141
30. Wang Y, Okada A, Moriya S, Hasebe Y (2010) Carbon felt-based bioelectrocatalytic flow detectors: covalent modification of tyrosinase onto a cyanuric chloride-activated carbon felt. Sensor Lett 8:677–683
31. Mason WT (1999) Fluorescent and luminescent probes for biological activity. Academic, London
32. Rodríguez-López JN, Ros JR, Varón R, García-Cánovas F (1993) Oxygen Michaelis constant for tyrosinase. Biochem J 293:859–866
33. Rodríguez-López JN, Tudela J, Varón R, García-Carmona F, García-Cánovas F (1992) Analysis of a kinetic model for melanin biosynthesis pathway. J Biol Chem 267:3801–3810
34. Naish-Byfield S, Riley PA (1992) Oxidation of monohydric phenol substrates by tyrosinase. An oximetric study. Biochem J 288:63–67
35. Naish-Byfield S, Cooksey CJ, Riley PA (1994) Oxidation of monohydric phenol substrates by tyrosinase: effect of dithiothreitol on kinetics. Biochem J 304:155–162
36. Ros JR, Rodríguez-López JN, García-Cánovas F (1993) Effect of L-ascorbic acid on the monophenolase activity of tyrosinase. Biochem J 295:309–312
37. Asuri P, Bale SS, Pangule RC, Shah DA, Kane RS, Dordick JS (2007) Structure, function and stability of enzymes covalently attached to single-walled carbon nanotubes. Langmuir 23:12318–12321

38. Roach P, Farrar D, Perry CC (2005) Interpretation of protein adsorption: surface-induced conformational changes. J Am Chem Soc 127:8168–8173
39. Chi Q, Zhang J, Nielsen JU, Friis EP, Chorkendorff I, Canters GW, Andersen JET, Ulstrup J (2000) Molecular monolayer and interfacial electron transfer of *Pseudomonas aeruginosa* Azurin on Au(111). J Am Chem Soc 122:4047–4055
40. Han E, Shan D, Xue H, Cosnier S (2007) Hybrid material based on chitosan and layered double hydroxides: characterization and application to the design of amperometric phenol biosensor. Biomacromolecules 8:971–975
41. Matulis D, Baumann CG, Bloomfield VA, Lovrien RE (1999) 1-Anilino-8-naphthalene sulfonate as a protein conformation tightening agent. Biopolymers 49:451–458
42. Celej MS, Montich GG, Fidelio GD (2003) Protein stability induced by ligand binding correlates with change in protein flexibility. Protein Sci 12:1496–1506
43. Williams DH, Stephens E, P.O'Brien D, Zhou M (2004) Understanding noncovalent interactions: ligand binding energy and catalytic efficiency from ligand-induced reductions in motion with receptors and enzymes. Angew Chem Int Ed 43:6596–6616
44. Ahmad A, Akhtar MS, Bhakumi V (2001) Monovalent cation-induced conformational change in glucose oxidase leading to stabilization of the enzyme. Biochemistry 40: 1945–1955
45. Lontie R (ed) (1984) Copper proteins and copper enzymes, vol 2. CRC Press, Boca Raton